Bcl-2 and N-Myc Coexpression Increases IGF-IR and Features of Malignant Growth in Neuroblastoma Cell Lines

Rama Jasty*, Cynthia van Golen[‡], Huey-Jen Lin[†], Gabe Solomon[†], Kathleen Heidelberger[§], Peter Polverini[¶], Anthony Opipari[#], Eva Feldman[‡] and Valerie P. Castle[†]

*Department of Pediatrics, Medical College of Ohio, Toledo, OH 43614; Department of [†]Pediatrics; [‡]Neurology; [§]Pathology; [¶]Dentistry; [#]Obstetrics and Gynecology, University of Michigan Medical School, Ann Arbor, MI 48109

Abstract

The *bcl-2* and c-*myc* oncogenes cooperate to transform multiple cell types. In the pediatric malignancy NB[2], Bcl-2 is highly expressed. In tumors with a poor prognosis, N-Myc, a protein homologous to c-Myc, is overexpressed as a result of gene amplification. The present study was designed to determine whether Bcl-2 cooperates with N-Myc to bestow a tumorigenic phenotype to neuroblastoma (NB) cells. NB cell lines that at baseline express neither Bcl-2 nor N-Myc were stably transfected to express these gene products. In this model, we found Bcl-2 rescues N-Myc–expressing cells from apoptosis induced by serum withdrawal. Coexpression of Bcl-2 and N-Myc supports growth in low serum conditions and anchorage-independent growth in soft agar. Similarly, *in vivo* tumorigenic and angiogenic activity was dependent on coexpression. Our data further suggests that the mechanism underlying these changes involves the receptor for insulin growth factor type I (IGF-IR).
Neoplasia (2001) **3,** 304–313.

Keywords: neuroblastoma, apoptosis, angiogenesis, tumorigenicity, N-Myc.

Introduction

Neuroblastoma (NB) is the most common extracranial solid tumor of children accounting for ∼10% of all childhood cancers [1]. The disease arises from sympathetic neuroblasts. Although the molecular defect(s) responsible for the genesis of NB is unknown, several biologic markers have been identified that correlate with disease outcome. N-*myc* gene amplification is the single best predictor of aggressive tumor growth and poor treatment outcome [2], implying this gene has an important role in pathogenesis. Nevertheless, N-*myc*'s molecular role in NB tumor behavior remains ill defined. N-Myc overexpression by single gene transfection advances the malignant phenotype of some human NB cells lines [3]. However, N-Myc overexpression also induces a predisposition to apoptosis in serum-deprived conditions [4]. The transforming and tumorigenic potential of the related *myc* family member, c-*myc* [5] depends on coexpression with *bcl-2* in hematopoietic and fibroblastic cell types [6–8]. As such it is plausible that N-*myc*'s oncogenic activity in NB requires the cooperation of other gene products, possibly Bcl-2.

Bcl-2 protein is detected in 40% to 100% of primary NB tumors and cell lines [9–11]. We and others have shown that in untreated human NB tumors, Bcl-2 expression correlates with N-*myc* amplification and unfavorable histology [9,12]. High levels of Bcl-2 are detected in residual tumor cells from patients who have persistent or recurrent disease following chemotherapy [9,13]. Targeted overexpression of Bcl-2 in NB cell lines decreases sensitivity to cytotoxic agents [14], further supporting a role in chemotherapy resistance.

A substantial fraction of NB tumors and cell lines overexpress N-Myc in the context of detectable Bcl-2. The behavior of NB tumors expressing both gene products might differ from those expressing either one or the other. Understanding whether these genes act cooperatively such that the oncogenic activity of one depends on the other would provide a further basis to stratify disease risk. Cooperative interplay has been observed between the N-*myc*–related genes c-*myc* and N-*myc2* in hematopoietic and murine hepatic cells, respectively [4,6–8]. We hypothesized that Bcl-2 expression facilitates N-Myc–induced transformation of NB cells. To test this hypothesis we stably transfected two human NB cell lines (SH-EP1 and SK-N-AS), which at baseline do not express detectable amounts of either Bcl-2 or N-Myc. Coexpression of Bcl-2 and N-Myc sustained growth in reduced serum, supported anchorage-independent growth and enhanced both angiogenic activity and *in vivo* tumorigenesis. Coexpression was associated with high-level insulin growth factor receptor type 1 (IGF-IR) expression further implicating this receptor system in the transformed phenotype of NB and providing mechanistic insight about the cooperative mechanism.

Materials and Methods

Cell Lines

The NB cell lines SMS-KCNR, SH-EP1, and SK-N-AS [15–17] were used in this study. SH-EP1 and SK-N-AS cell lines do not express detectable levels of Bcl-2 or N-Myc by Western analysis (Castle, unpublished observations). The SMS-KCNR NB line is N-*myc* amplified, expresses Bcl-2 and is tumorigenic in xenograft models. An NIH-3T3 cell line transformed by v-*src* was used as a positive control in soft agar assays. Cells were maintained in minimum essential medium (MEM) or RPMI-1640 (Sigma-Aldrich, St. Louis, MO) supplemented with 10% fetal bovine serum (FBS), 2 mM glutamine, 10 U/ml penicillin and 100 μg/ml streptomycin. Following transfection, cells were cultured in the same medium supplemented with G418 (Life Technologies, Rockland, MD) at 500 μg/ml.

Transfections

The SH-EP1 and SK-N-AS lines were stably transfected to generate four expression phenotypes: Bcl-2 alone, N-Myc alone, Bcl-2/N-Myc, or vector control. Expression plasmids used for these studies were p*SSFVneo-bcl-2*; vector p*SSFVneo* [18] (gift of Gabriel Nuñez, University of Michigan); p*CMV-N-myc* and vector p*SMneo* [19] (gift of William Fahl, McArdle Laboratory for Cancer Research, Madison WI). Clones designated vector control were simultaneously transfected with both empty vector plasmids. Transfections were performed using lipofectamine according to the manufacturer instructions (Gibco, Grand Island, NY). Briefly, 5×10^4 cells were plated in serum-free medium and transfected with 10 μg of plasmid DNA. Forty-eight hours later, cells were transferred to 100-mm plates and selected in G418. G418-resistant colonies were transferred by filter paper and subcultured individually. The resulting G418-resistant colonies expressed variable levels of both Bcl-2 and N-Myc protein. The clones chosen for further study expressed the highest levels of both proteins, similar to the control KCNR cell line.

Detection of Bcl-2, N-Myc, and IGF-IR by Western Analysis

The expression of Bcl-2, N-Myc, and IGF-IR was determined by Western analysis using the enhanced chemiluminescence technique (ECL detection kit, Amersham International, Buckinghamshire, UK). Cells were harvested and lysed in a buffer containing 50 mM Tris–HCL, 100 mM dithiothreitol, 2% SDS, 0.1% bromphenol blue, and 10% glycerol. Protein was quantified using a Bradford assay (BioRad Laboratories, Hercules, CA). Protein was electophoretically resolved on 12% SDS–polyacrylamide gels and transferred to nitrocellulose by electroblotting. Proteins were detected with either hamster monoclonal antibody to N-Myc (AB-1, Oncogene Science, San Diego, CA), a polyclonal antibody to Bcl-2 (6C8, Pharmingen, San Diego, CA), a polyclonal antibody to IGF-IR (Santa Cruz Biotechnology, Santa Cruz, CA) or a monoclonal antibody for glyceride-3-phosphate dehydrogenase (GAPDH, Chemicon, Temacula, CA).

Cell Growth and Viability

Cells (5×10^4) were suspended in growth medium containing 1% FBS in wells on 96-well plates. Growth medium was replaced every other day for the duration of the experiment. Cell viability and number was assessed using the MTT assay [20] using a lysis buffer containing 2% SDS, 50% *N,N*-dimethylformamide (pH 4.5). Absorbance at 570 nM (Abs_{570}) was determined for each well using an ELX 808 automated microplate reader (Bioteck Instruments, Winnoski, VT). After subtracting for background absorbance of the medium, the viability of each cell line was expressed as the viable cell index [VCI = (Abs_{570} on consecutive days/Abs_{570} on day 0) $\times$ 100]. Data is presented as the mean and standard deviation (SD) of multiple experiments.

Independent Colony Growth in Soft Agar

Cells (10^4) were plated in triplicate in 2 ml of 0.33% low melting point agarose (Seaplaque, FMC, Rockland, ME) in MEM containing 10% FBS, 2 mM glutamine, 100 U/ml penicillin, and 100 mg/ml streptomycin, over 0.9% bottom agar plates prepared in the same medium. Plates were incubated at 37°C in a humidified 5% CO_2 incubator. Foci were scored as colonies if the collection of cells could be visualized without microscopic aid 14 days after plating.

Tumorigenicity in Athymic Mice

In vivo growth of tumor cells was determined in female Swiss athymic mice (Charles River Laboratories, Raleigh, NC) as previously described [21]. After routine culture, cells were harvested by trypsinization and suspended in a total volume of 100 μl with serum-free MEM. The cell suspension was injected into the anterior thigh musculature. Mice were observed three times per week over 90 days to detect tumors and volumes estimated on the basis of two dimensions as previously reported [22]. After sacrifice, tissue was prepared for histologic analysis.

Quantification of Microvessels in Tumor Specimens

Microvessels were identified in tissue sections by immunostaining for endothelial cells with antimouse PECAM-1 (CD31). Formalin-fixed, paraffin-embedded tissues mounted on glass slides were deparaffinized and quenched in 0.3% H_2O_2 in methanol to block endogenous peroxidase. Antigen retrieval was accomplished by heating tissue sections in citrate buffer (pH 6.0) for 10 minutes and placing sections in a 1100-W microwave oven on full power for an additional 10 minutes. Sections were cooled to room temperature, washed with buffer and incubated with normal mouse serum (1:200) for 30 minutes. Slides were incubated with primary antibody (rabbit antimouse CD31, 1:10, Dako, Carpinteria, CA) overnight at 37°C, then with secondary antibody (biotinylated goat antirabbit IgG, 1:500) for 30 minutes, followed by a 30-minute incubation

with avidin−biotin−horseradish peroxidase complex (ABC, Vector Laboratories, Burlingame, CA). Color development was done with 3-amino 9-ethyl carbazole treatment followed by counterstain with Gill's hematoxylin. As a negative control, sections were treated with secondary antibody alone. Microvessels were quantitated by a modification of the method of Weidner et al. [23]. Sections were examined under low magnification to identify the regions of highest vessel density and the vessel counts in each of 10 high power fields (HPF) (400×) were determined. A vessel lumen was not required for identification of a microvessel; cell clusters were counted. Vessel counts were obtained from a minimum of three different sections per tumor and expressed as the mean number per 10 HPF.

Assessment of Angiogenic Activity in Conditioned Medium

The rat micropocket assay was used to assess angiogenic activity of conditioned medium as previously described [24]. Conditioned medium was concentrated 5- to 10-fold using Centricon spin columns (3000 MW, Millipore, Bedford, MA) to a protein concentration of 1 μg/5 μl. Equal volumes of concentrated medium and Hydron casting solution were combined. Ten microliters of the resulting solution was dispensed atop the surface of 1-mm-diameter Teflon rods (Dupont, Wilmington, DE) and air-dried in a laminar flow hood. Dried pellets were rehydrated with phosphate-buffered saline and implanted into surgically created pockets in the eyes of Fisher strain rats. Animals were examined daily to monitor vessel response. After 7 days, rats were perfused with colloidal carbon to enumerate new corneal vessels. After enucleation, corneas were excised, fixed in 10% formalin, and photographed. Positive neovascular responses were recorded when a brush-like network of capillary sprouts and hairpin loops were observed extending from the limbus toward the implant. Negative responses were recorded if only an occasional capillary sprout with no evidence of sustained growth was observed or when no growth was detected. Corneal responses were quantified by measuring the area occupied by new capillaries and venules using NIH Image software. Corneal mounts were photographed and digitized into Adobe PhotoShop 5.0. The area occupied by new vessels was captured with NIH Image and the results were expressed as the area in pixels. At least three corneas were evaluated per cell line and the results shown as mean values with standard deviation.

Statistics

The Fisher's exact test was used to determine statistical significance unless otherwise indicated.

Results

Generation of Bcl-2− and N-Myc−Expressing NB Cell Lines

To determine whether Bcl-2 cooperates with N-Myc to enhance the tumorigenicity of NB, two NB cell lines (SH-

EP1 and SK-N-AS) were stably transfected to express Bcl-2, N-Myc, or both gene products. Whereas the SH-EP1 and SK-N-AS lines express no detectable Bcl-2 or N-Myc at baseline, multiple unique transfectants were found that express levels of Bcl-2 and N-Myc comparable to the control SMS-KCNR NB cell line (Figure 1).

Bcl-2 and N-Myc Coexpression Confers Serum- and Anchorage-Independent Growth Characteristics

SH-EP1 and SK-N-AS cells expressing Bcl-2, N-Myc, or both gene products were cultured in reduced serum media. Under these conditions, neither parental line was able to proliferate (Figure 2). Transfectants expressing only Bcl-2 similarly had no proliferative capacity. N-Myc expression in SK-N-AS cells resulted in cell death evidenced by a decrease in cell number after 2 to 6 days. Even though the viability of N-Myc−expressing SH-
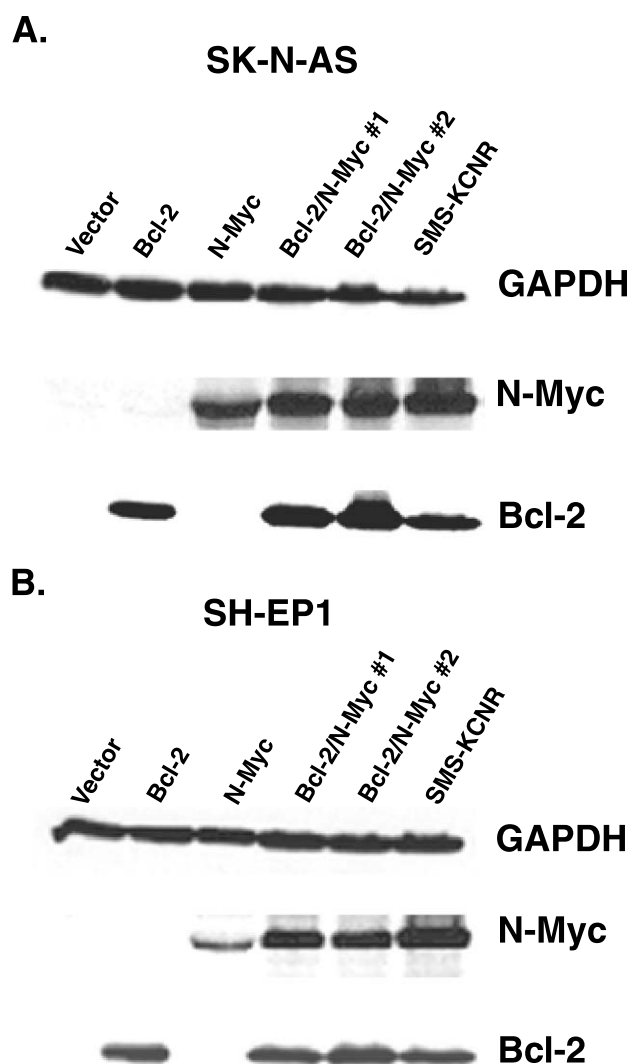
Figure 1. Immunoblot analysis of SH-EP1 and SK-N-AS transfectants for Bcl-2 and N-Myc expression. The Bcl-2 and N-My−expressing SMS-KCNR cell line was used as a positive control. Equivalent protein loading is confirmed by GAPDH detection.
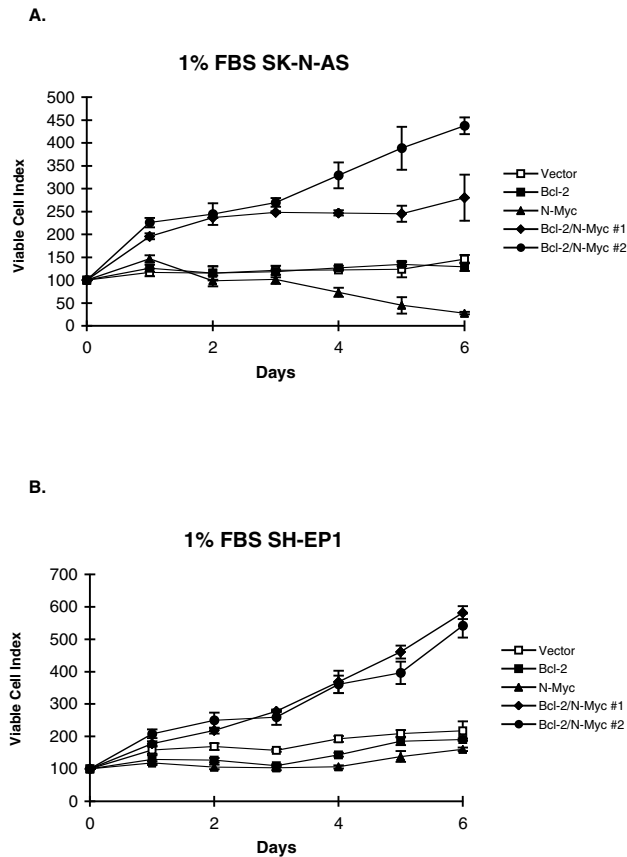
A.

B.

Figure 2. *Relative viability after culture in medium with 1% serum was determined by MTT for (A) SK-N-AS and (B) SH-EP1 transfectants. Data presented as the mean and standard deviation from three separate experiments.*

EP1 cells did not similarly decrease in low serum, TUNEL revealed increased apoptosis in both SH-EP1 and SK-N-AS cells overexpressing N-Myc when compared to vector controls (data not shown). Most dramatically, coexpression of Bcl-2 and N-Myc (in multiple unique clones) provides each parental cell type the ability to proliferate in serum deprived culture conditions.

Anchorage-independent growth was observed only in those transfectants that coexpressed Bcl-2 and N-Myc (Figure 3, Table 1). Vector control lines or SH-EP1 and SK-N-AS cells expressing Bcl-2 or N-Myc alone did not grow in soft agar. All transfected clones coexpressing Bcl-2 and N-Myc produced soft agar colonies at a plating efficiency that approached that of the highly transformed v-src NIH-3T3 positive control line.

Bcl-2 and N-Myc Cooperate to Induce Tumors in Animals

We tested the transfected cell lines to determine tumorgenic potential in a mouse xenograft model. Cells of each transfectant [(1 and 2)$\times 10^7$] as well as the SMS-KCNR positive control line were inoculated into athymic mice (Figure 4A). All animals inoculated with either dose of SMS-KCNR control cells formed palpable tumors within 26 days. In contrast, SH-EP1 and SK-N-AS vector control lines formed no tumors during the experimental course (90

days). Similarly, SH-EP1 cells expressing either Bcl-2 or N-Myc formed no tumors. However, cells expressing both Bcl-2 and N-Myc were tumorigenic with the take rate increasing with inoculated cell number. Thirty-three percent of mice receiving 1×10^7 cells formed tumors whereas 65% injected with 2×10^7 cells formed tumors. SK-N-AS cells transfected to express Bcl-2, N-Myc, or the two together also formed tumors. At the lower inoculum (1×10^7 cells) 100% of mice injected with SK-N-AS Bcl-2/N-Myc cells formed tumors as compared with 33% injected with the same inoculum of SH-EP1 Bcl-2/N-Myc−expressing cells (*P*<.001).

The growth characteristics of the SK-N-AS Bcl-2 tumors were significantly different from the SK-N-AS N-Myc and SK-N-AS Bcl-2/N-Myc tumors: the latency to tumor formation was 61 days *vs* 13 to 27 days and the time to triple 74 days *vs* 25 to 33 days (*P*<.05). The growth characteristics of the SH-EP1 Bcl-2/N-Myc lines were similar to the SK-N-AS Bcl-2 line. The SH-EP1 Bcl-2/N-Myc tumors were recognized after 54 to 78 days and tripled in size by 72 days. There was a statistically significant difference in take rate, latency, and time to triple between the SH-EP1 Bcl-2/N-Myc and SK-N-AS Bcl-2/N-Myc lines (*P*<.001). These results suggest Bcl-2 and N-Myc cooperate to enhance the tumorigenicity of NB cells. However, the impact of coexpression on *in vivo* growth characteristics varies between parental cell types suggesting other factors influence this cooperative interplay.

Histologic Analysis of Xenograft Tumors

The histologic appearance of the SH-EP1 and SK-N-AS tumors was similar (Figure 4B). As well, there were no distinguishing features between Bcl-2/N-Myc, Bcl-2 alone, or N-Myc alone tumors. All tumors had a biphasic phenotype. They were variably necrotic with morphologic features of sarcomatous and chondroblastic differentiation. Some tumors showed hyperchromatic background cells with limited amounts of amphophilic cytoplasm, round to oval nuclei and prominent eosinophilic, and generally single nucleoli. Abnormal mitotic figures were abundant. The more epithelial appearing areas included cells with abundant eosinophilic cytoplasm and variable shape. Unlike human NB tumor specimens, tumors from the transfectants showed no neuropile, rosetting, or stroma formation.

Tumor Microvasculature and Angiogenic Activity

Tumor microvasculature was examined to determine if angiogenic activity correlates with the differences in tumorigenicity observed between the SH-EP1 and SK-N-AS transfectants. The greatest angiogenic response was seen in S-K-AS Bcl-2/N-Myc tumors (Figure 5). Vessel counts in these tumors were similar to counts in positive control SMS-KCNR tumors. Tumors from SK-N-AS Bcl-2 and SK-N-AS N-Myc single transfectants had approximately 50% as many vessels as SK-N-AS Bcl-2/N-Myc tumors. Vessel counts
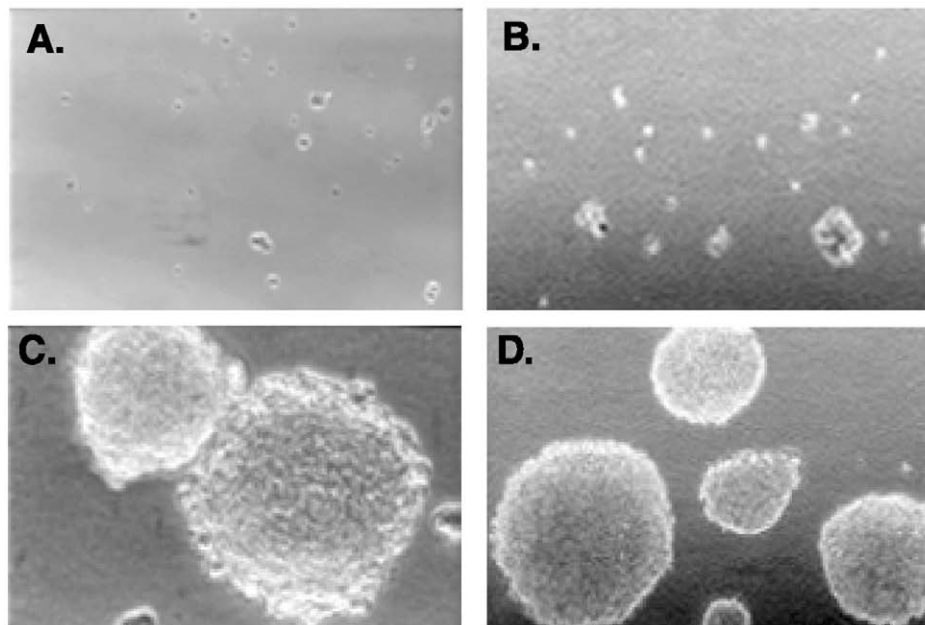
Figure 3. *Soft agar growth observed under 10× magnification of foci from (A) SH-EP1 vector, (B) SK-N-AS N-Myc, (C) SH-EP1 Bcl-2/N-Myc and (D) SK-N-AS Bcl-2/N-Myc.*

from SH-EP1 Bcl-2/N-Myc tumors were significantly lower than the SK-N-AS Bcl-2/N-Myc counterparts ($P < .001$).

To further extend the evaluation of angiogenic activity to include the transfected lines that did not produce tumors (SH-EP1 Bcl-2 and SH-EP1 N-Myc), *in vitro* angiogenic activity was assessed in rat corneas. Vector-transfected controls failed to induce a neovascular response (Figure 6, *A* and *C*). SH-EP1 Bcl-2/N-Myc and SK-N-AS Bcl-2/N-Myc lines induced a response (Figure 6, *A* and *B*). Neovascularization was established as early as 3 days after pellet implantation with further growth and recruitment of additional new capillaries throughout the 7-day assay period. Significant neovascular responses were also detected from each of the single gene transfectants. The responses from each of these cell types were nearly equivalent and significantly less than that observed for cells

Table 1. Anchorage-Independent Soft Agar Colony Formation.

Parental Cell Line	Clone	Colonies*
NIH-3T3	v-src	1000
	vector	0
SH-EP1	N-Myc	0
	Bcl-2	5
	Bcl-2/N-Myc #1	471
	Bcl-2/N-Myc #2	420
	vector	0
SK-N-AS	N-Myc	0
	Bcl-2	0
	Bcl-2/N-Myc #1	580
	Bcl-2/N-Myc #2	450

*Colonies per 10^4 plated cells. Average of three replicate experiments.

expressing both Bcl-2 and N-Myc. These results are most consistent with Bcl-2 and N-Myc independently increasing angiogenic activity, although their coexpression results in an additive response. *In vitro* angiogenic activity does not predict tumorigenic behavior because the nontumorigenic SH-EP1 single gene transfectants induced an angiogenic response equivalent to their tumorigenic SK-N-AS counterparts.

Bcl-2 and N-Myc Increase IGF-IR Expression

To understand the process by which coexpression enhanced the transformation of NB cells (acquisition of serum and anchorage-independent growth, tumorigenicity) we examined the effects on the IGF-IR signaling pathway (Figure 7). IGF-IR was chosen, as it is known to support the growth and chemotaxis of NB cells [25–27]. IGF-IR expression was undetectable in SH-EP1 vector–transfected and SH-EP1 Bcl-2–expressing lines. SH-EP1 cells expressing N-Myc alone show slight IGF-IR expression. However, SH-EP1 cells expressing Bcl-2/N-Myc show substantial IGF-IR expression. In contrast to SH-EP1 cells, SK-N-AS vector controls express some (low basal level) IGF-IR. IGF-IR is increased in SK-N-AS cells expressing only Bcl-2, only N-Myc, and in cells expressing both Bcl-2 and N-Myc. These data suggest a relationship between induced IGF-IR expression and tumorigenicity. Each of the tumorigenic clones expressed IGF-IR. IGF-IR is dramatically induced in SH-EP1 cells when Bcl-2 and N-Myc are coexpressed reflecting the cooperative action of these gene products. As presented above, cooperation was also necessary for tumorigenesis in SH-EP1 cells. In SK-N-AS cells, either Bcl-2 or N-Myc induces IGF-IR without any further increase caused by coexpression. Similar to these findings, cooperativity

A.

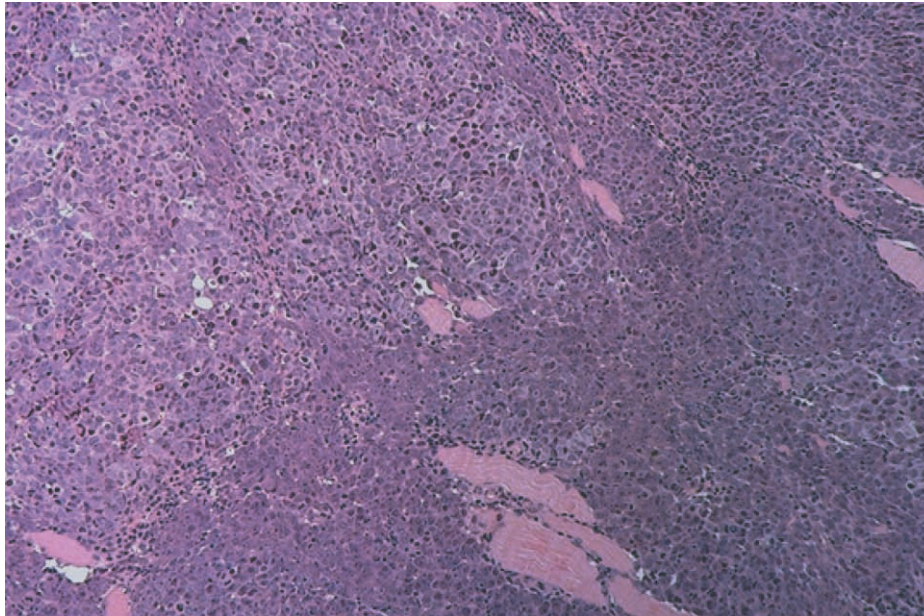| Parental Line	Transfected Clone/Inoculum	No Tumor	Tumor	Latency (days)
SH-EP1	vector 1x10^7	ooo ooo		
	vector 2x10^7	oo ooo		
	N-Myc 2x10^7	oo ooo ooo		
	bcl-2 2x10^7	oo ooo		
	bcl-2/N-Myc 1x10^7	ooo ooo	●●●	51-78
	bcl-2/N-Myc 2x10^7	ooo	● ●●●	43-54
SK-N-AS	vector 2x10^7	oo ooo		
	N-Myc 1x10^7	o	●●	24-27
	N-Myc 2x10^7		●●●	18-21
	bcl-2 2x10^7	o	●●	61
	bcl-2/N-Myc 1x10^7		●● ●●●	13-23
	bcl-2/N-Myc 2x10^7		●● ●●●	16-24

B.

Figure 4. *(A) Frequency plot of tumor formation in athymic mice. Mice were inoculated with (1 or 2)×10^7 cells and tumors determined by palpation. (B) Representative micrograph of H and E stained tumor specimen (25×) from SH-EP1 Bcl-2/N-Myc tumor highlighting biphasic phenotype.*

appeared to play a minor role in the tumorigenic behavior of SK-N-AS cells.

Discussion

The capacity of *bcl-2* to cooperate with c-*myc* to enhance tumor growth is established in lymphoma and mammary carcinoma [28,29]. We hypothesized that a similar cooperative relationship exists between *bcl-2* and N-*myc*. NB provides an important model to assess whether cooperation between *bcl-2* and N-*myc* contributes to oncogenesis,

because NB tumor specimens and cell lines commonly express both of these genes [9,12,30]. In NB, it is well known that N-Myc overexpression through gene amplification predicts aggressive malignant disease. However, not all N-Myc overexpressing tumors present with unfavorable histology or fail treatment [31]. Furthermore, in a transgenic mouse model, N-Myc overexpression produced clonal NB-like tumors after considerable latency, reflecting a requirement for other genetic alterations as second hits [32]. These observations suggest that N-Myc expression alone in NB is insufficient to bestow a malignant phenotype. Rather,
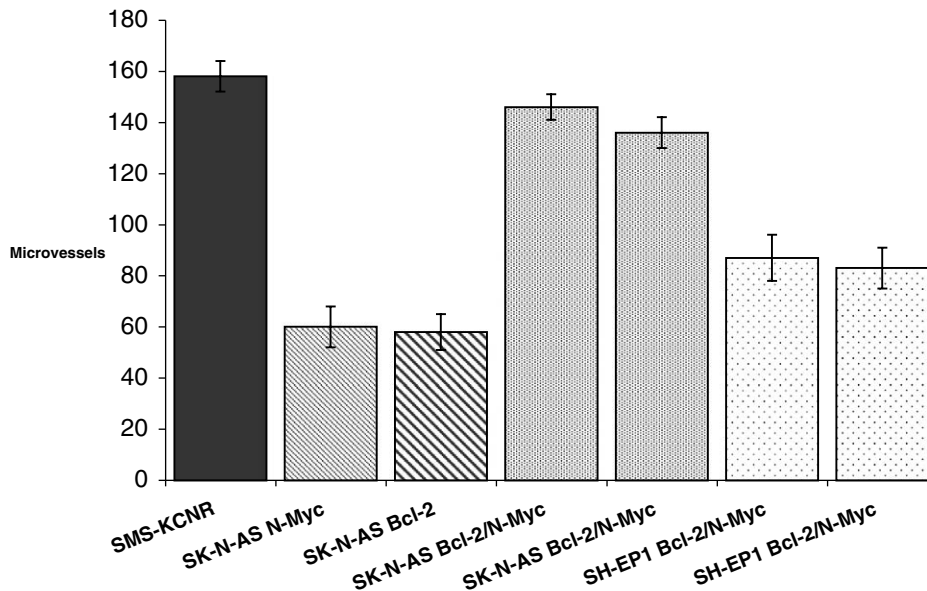
Figure 5. *Microvessel counts of tumors. Two unique SH-EP1 and SK-N-AS transfected cell lines expressing N-Myc and Bcl-2 each formed tumors in nude mice. At sacrifice, tumors were resected and microvessels quantified by CD31 expression. Data presented as mean vessels/10 HPF.*

aggressive tumor behavior likely depends on other specific gene products that act cooperatively with N-Myc.

Our data establishes that coexpression of Bcl-2 and N-Myc in NB cells furthers the malignant phenotype. *In vitro* growth in low serum or in soft agar is particularly dependent on coexpression as the same dependency was observed for both cell lines evaluated. Coexpression was necessary for SH-EP1 cells to become tumorigenic in the xenograft model. Conversely, in the SK-N-AS line single gene expression of N-Myc or Bcl-2 was sufficient for tumor growth, revealing an important difference between SH-EP1 and SK-N-AS cells with respect to their ability to acquire malignant features. In the SK-N-AS cells coexpression appears to increase tumorigenicity above that achieved with either gene product alone. Thus on the basis of the SK-N-AS results it appears that coexpression of N-Myc and Bcl-2 is not always required for NB tumorigenesis. It also must be recognized that our results do not conclusively exclude the possibility that SH-EP1 single gene transfectants can form tumors. For example, tumors may have formed if inoculated cell number was significantly increased or tumors may have formed at a frequency below that detectable with the number of mice used in this study. To summarize, coexpression convincingly increased the malignant phenotype beyond that achieved with either gene alone in SH-EP1 cells. Coexpression appears to increase tumorigenicity in SK-N-AS cells (particularly at the 1×10^7 inoculum); however, larger sample size would be necessary to conclude this definitively.

SK-N-AS cell survival in low serum is compromised by N-Myc expression in the absence of Bcl-2. Mechanistically, this finding may highlight one basis for the cooperativity between these gene products. Studies with c-*myc* have similarly revealed that its expression under conditions of growth factor deprivation induces apoptosis [33] and that Bcl-2 is able to rescue these cells from death [7–9]. Thus, it

appears cooperation between Bcl-2 and N-Myc emerges from the ability of Bcl-2 to overcome the pro-apoptotic action of N-Myc expression. These observations offer further support for the hypothesis proposed by Cory et al. [34] that synergy between oncogenes results from the ability of one to counter the antioncogenic impulses of the other. Despite extensive study, the mechanism underlying the oncogenic activity of c-*myc* (and N-*myc* as well) remains ill defined. The activity of *myc* genes has been linked to increased proliferation and cell cycle progression (reviewed in Cole and McMahon [35]). Indeed the mechanism by which c-*myc* induces apoptosis appears to be closely associated with its effects on the cell cycle (reviewed in Thompson [36]). In our system, N-Myc is likely providing cells an increased proliferative capacity possibly through transcriptional activation of cyclin Dl/*bcl-1* as described for c-*myc* [37]. Under low serum conditions, this proliferative response may trigger apoptotic signals that are blocked when Bcl-2 is coexpressed.

Multiple cellular processes must converge to allow establishment and growth of a tumor within an animal. Not surprisingly properties in addition to proliferative capacity and resistance to apoptosis are required. Paramount among these is the tumor cell's ability to recruit and support new blood vessels, termed angiogenesis. In human tumors N-*myc* amplification has been associated with an increased vascular index that independently predicts poor outcome [38]. Tumor microvessel counts were higher in SK-N-AS coexpressing tumors compared to SH-EP1 coexpressing tumors. This difference corresponds with the increased tumorigenicity of the SK-N-AS Bcl-2/N-Myc cells. Comparison of the vascularity in SK-N-AS coexpressing tumors to SK-N-AS tumors expressing Bcl-2 or N-Myc alone reveals that coexpression results in increased tumor blood vessels. This response provides support for the concept of
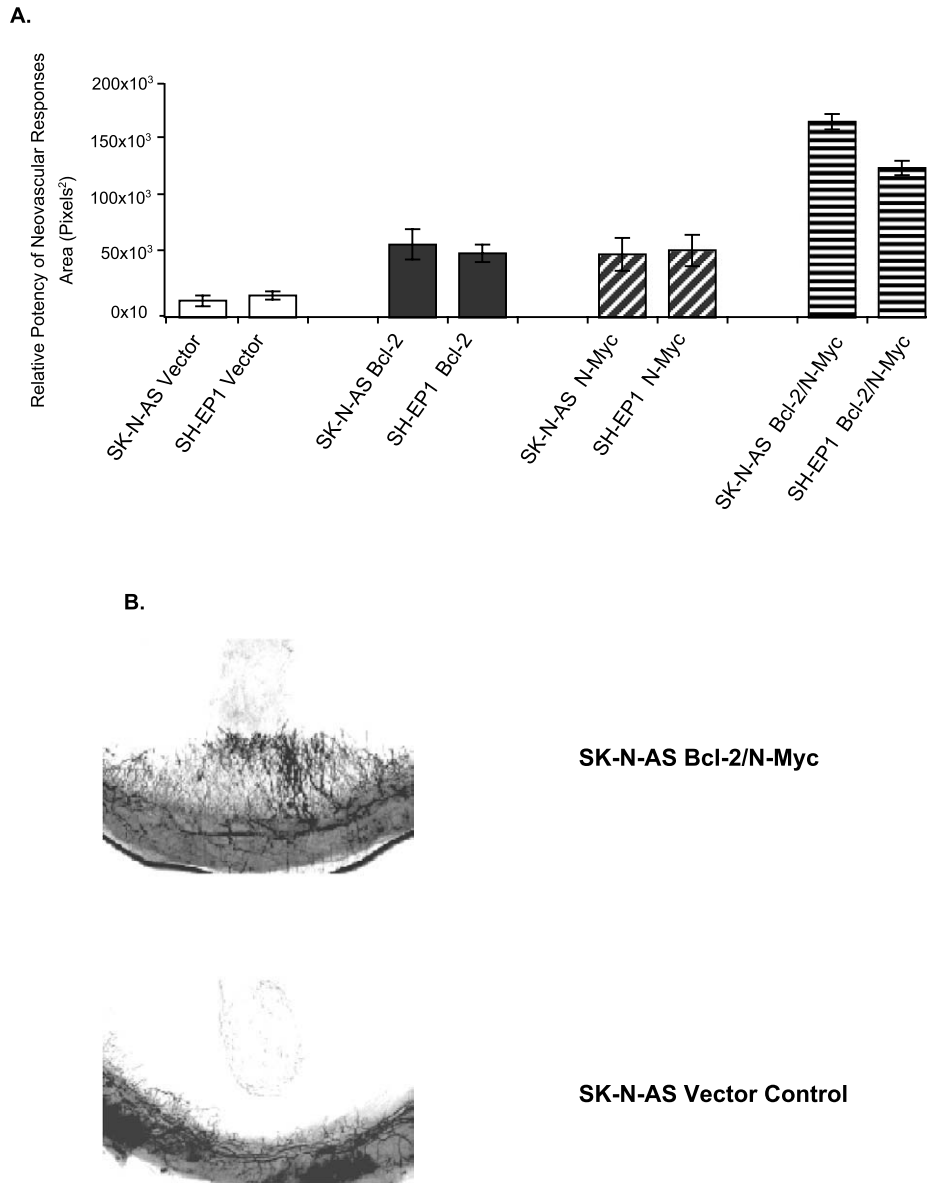
A.

B.

SK-N-AS Bcl-2/N-Myc

SK-N-AS Vector Control

Figure 6. *Neovascular response from conditioned medium derived from cultured SH-EP1 and SK-N-AS transfectants in the rat corneal implant assay. (A) Quantification of microvessels by pixel counts showing mean and standard deviation of three separate experiments. Photomicrographs of the response following treatment with conditioned medium from (B) SK-N-AS Bcl-2/N-Myc and (C) SK-N-AS vector control cells.*

cooperative action of these oncogenes in the SK-N-AS cell model. Rat cornea angiogenic responses to conditioned media revealed that expression of either Bcl-2 or N-Myc increased angiogenic activity from control and that coexpression led to a further additive increase. These results demonstrate angiogenic activity results from the expression of either N-Myc or Bcl-2 through independent processes that appear to not require the presence of the other gene product.

NB tumor growth is supported by autocrine and paracrine stimulation through IGF-IR [25,26]. Inhibition of IGF-IR expression blocks NB tumor behavior in mice [39]. By binding to IGF-IR, IGF-I induces morphologic changes that are associated with migration and chemotaxis of NB cells [27] and protects NB cells from apoptosis [40–42]. N-Myc overexpression in NB cells leads to increased expression of

several components of the IGF system including IGF-II, IGF-IR, IGFBP-2, and IGFBP-4 [43]. In a reciprocal fashion IGF-I itself induces N-*myc* mRNA and protein expression [44]. The mutual interdependence of these gene products prompted these authors to suggest a hypothesis whereby IGF-IR and N-Myc upregulate each other. In this situation, a positive feedback loop would likely contribute to aberrant cell behavior and tumorigenicity.

Because the IGF ligands signal through IGF-IR, we sought to determine whether the differences in the tumorigenic phenotype exhibited by the SH-EP1 and SK-N-AS Bcl-2/N-Myc−expressing lines were related to differences in IGF-IR expression. SH-EP1 cells express very little IGF-IR and no IGF-I or IGF-II ligands [42]. SK-N-AS cells express both IGF-IR and IGF-II, which support autonomous growth of these cells in culture [45]. In the current study,
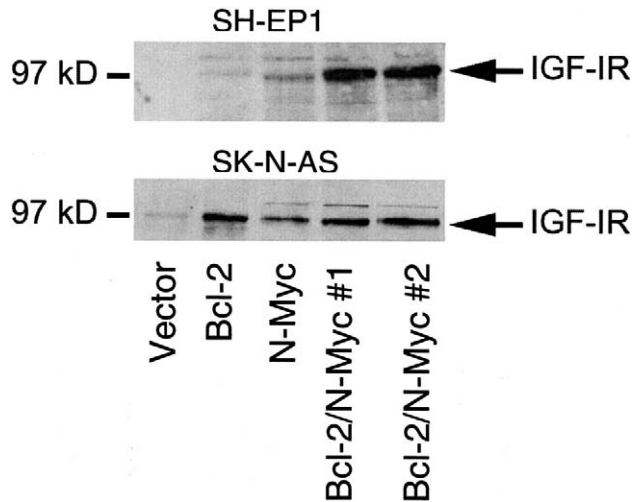
Figure 7. *IGF-IR expression in SH-EP1 and SK-N-AS transfectants. IGF-IR is detected as a 97-kDa band. IGF-IR is undetectable in SH-EP1 vector or Bcl-2 expressing cells and barely detectable in the SH-EP1 N-Myc line. Coexpression of Bcl-2 and N-Myc in SH-EP1 cells results in a dramatic increase in IGF-IR. SK-N-AS vector control cells express detectable IGF-IR that is increased with overexpression of Bcl-2, N-Myc, or Bcl-2/N-Myc.*

expression of either Bcl-2 or N-Myc slightly increases IGF-IR expression in SH-EP1 cells. Dramatic increases in IGF-IR resulted when both Bcl-2 and N-Myc were expressed. In contrast, Bcl-2 or N-Myc overexpression alone increased IGF-IR in SK-N-AS cells. Thus, as is true for tumorigenicity, Bcl-2 and N-Myc act cooperatively in SH-EP1 cells to induce IGF-IR. In SK-N-AS cells, no evidence is seen for cooperative induction of this receptor. In our results, all tumor-forming cell lines expressed IGF-IR. This finding begins to provide evidence that IGF-IR expression is important in NB tumorigenesis. Further characterization of additional NB cell lines with respect to IGF-IR expression and tumorigenicity would be helpful to determine if indeed IGF-IR expression is necessary for tumor growth.

In summary, our studies demonstrate Bcl-2 cooperates with N-Myc to influence the growth characteristics and tumorigenicity of NB cells. The coexpression of Bcl-2 and N-Myc influences the vascularity of tumors and together they enhance the angiogenic response *in vitro*. It is possible that these findings are related to changes in growth factor responses resulting through the upregulation of IGF-IR.

References

[1] Brodeur G, Castleberry R, Pizzo P, and Poplack D. (1993). Principles and Practice of Pediatric Oncology. J.B. Lippincott, Philadelphia, PA. pp. 739–767.

[2] Brodeur G, Seeger R, Schwab M, Varmus H, and Bishop J (1984). Amplification of N-myc in untreated human neuroblastomas correlates with advanced disease stage. *Science* **224**, 1121–1124.

[3] Schweigerer L, Breit S, Wenzel A, Tsunamoto K, Ludwig R, and Schwab M (1990). Augmented MYCN expression advances the malignant phenotype of human neuroblastoma cells: evidence for induction of autocrine growth factor activity. *Cancer Res* **50**, 4411–4416.

[4] Ueda K, and Ganem D (1996). Apoptosis is induced by N-myc expression in hepatocytes, a frequent event in hepadnavirus oncogenesis, and is blocked by insulin-like growth factor II. *J Virol* **70**, 1375–1383.

[5] Kohl NE, Legouy E, DePinho RA, Nisen PD, Smith RK, Gee Ce, and Alt FW (1986). Human N-myc is closely related in organization and nucleotide sequence to c-myc. *Nature* **319**, 73–77.

[6] Vaux D, Cory S, and Adams J (1988). Bcl-2 gene promotes haemopoietic cell survival and cooperates with c-myc to immortalize pre-B cells. *Nature* **335**, 440–442.

[7] Bissonnette RP, Echeverri F, Mahboubi A, and Green DR (1992). Apoptotic cell death induced by c-myc is inhibited by bcl-2. *Nature* **359**, 552–554.

[8] Fanidi A, Harrington EA, and Evan GI (1992). Cooperative interaction between c-myc and bcl-2 proto-oncogenes. *Nature* **359**, 554–556.

[9] Castle VP, Heidelberger KP, Bromberg J, Ou X, Dole M, and Nunez G (1993). Expression of the apoptosis-suppressing protein bcl-2, in neuroblastoma is associated with unfavorable histology and N-myc amplification. *Am J Pathol* **143**, 1543–1550.

[10] Ikeda H, Hirato J, Akami M, Matsuyama S, Suzuki N, Takahashi A, and Kuroiwa M (1995). Bcl-2 oncoprotein expression and apoptosis in neuroblastoma. *J Pediatr Surg* **30**, 805–808.

[11] Reed JC, Meister L, Tanaka S, Cuddy M, Yum S, Geyer C, and Pleasure D (1991). Differential expression of bcl2 protooncogene in neuroblastoma and other human tumor cell lines of neural origin. *Cancer Res* **51**, 6529–6538.

[12] Mejia MC, Navarro S, Pellin A, Castel V, and Llombart-Bosch A (1998). Study of bcl-2 protein expression and the apoptosis phenomenon in neuroblastoma. *Anticancer Res* **18**, 801–806.

[13] Krajewski S, Chatten J, Hanada M, and Reed JC (1995). Immunohistochemical analysis of the Bcl-2 oncoprotein in human neuroblastomas. *Lab Invest* **72**, 42–54.

[14] Dole M, Nunez G, Merchant AK, Maybaur J, Rode CK, Bloch CA, and Castle VP (1994). Bcl-2 inhibits chemotherapy-induced apoptosis in neuroblastoma. *Cancer Res* **54**, 3253–3259.

[15] Helson L, Member B, and Helson C (1984). Importance of clinical exposure on verapamil enhancement of adriamycin–vincristine cytotoxicity in human neuroblastoma. *Cancer Drug Delivery* **1**, 303–305.

[16] Reynolds CP, Biedler JL, Spengler BA, Reynolds DA, Ross RA, Frenkel EP, and Smith RG (1986). Characterization of human neuroblastoma cell lines established before and after therapy. *J Natl Cancer Inst* **76**, 375–387.

[17] Sugimoto T, Tatsumi E, Kemshead J, Helson L, Green A, and Minowada J (1984). Determination of cell surface membrane antigens common to both human neuroblastoma and leukemia-lymphoma cell lines by a panel of 38 monoclonal antibodies. *J Natl Cancer Inst* **73**, 51–57.

[18] Hockenbery D, Nuñez G, Milliman C, Schreiber RD, and Korsmeyer SJ (1990). Bcl-2 is an inner mitochondrial membrane protein that blocks programmed cell death. *Nature* **348**, 334–336.

[19] Brondyk WH, Boeckman FA, and Fahl WE (1991). N-myc oncogene enhances mitogenic responsiveness of diploid human fibroblasts to growth factors but fails to immortalize. *Oncogene* **6**, 1269–1276.

[20] Hansen MB, Neilson SE, and Berg K (1989). Re-examination and further development of a precise and rapid dye method for measuring cell growth and cell kill. *J Immunol Methods* **119**, 203–210.

[21] Castle V, Varani J, Fligiel S, Prochownik EV, and Dixit V (1991). Antisense-mediated reduction in thrombospondin reverses the malignant phenotype of a human squamous carcinoma. *J Clin Invest* **87**, 1883–1888.

[22] Cozzutto C, and Cornaglia-Ferraris P (1991). Pleomorphic (anaplastic) neuroblastoma in nude mice. *Arch Pathol Lab Med* **115**, 68–73.

[23] Weidner N, Semple J, Welch W, and Folkman J (1991). Tumor angiogenesis and metastasis — correlation in invasive breast carcinoma. *N Engl J Med* **324**, 1–8.

[24] Rastinejad F, Polverini PJ, and Bouck NP (1989). Regulation of the activity of a new inhibitor of angiogenesis by a cancer suppressor gene. *Cell* **56**, 345–355.

[25] Martin DM, Singleton JR, Meghani MA, and Feldman EV (1993). IGF receptor function and regulation in autocrine human neuroblastoma cell growth. *Regul Pept* **48**, 225–232.

[26] Leventhal PS, Randolph AE, Vesbit TE, Schenone A, Windebank A, and Feldman E (1995). Insulin-like growth factor-II as a paracrine growth factor in human neuroblastoma cells. *Exp Cell Res* **221**, 179–186.

[27] Puglianiello A, Germani D, Rossi P, and Cianfarani S (2000). IGF-I stimulates chemotaxis of human neuroblasts. Involvement of type 1 IGF receptor, IGF binding proteins, phosphatidylinositol-3 kinase pathway and plasmin system. *J Endocrinol* **165**, 123–131.

[28] Marin MC, Hsu B, Stephens LC, Brisbay S, and McDonnell TJ (1995). The functional basis of c-myc and bcl-2 complementation during multistep lymphomagenesis *in vivo*. *Exp Cell Res* **217**, 240–247.

[29] Jager R, Herzer U, Schenkel J, and Weiher H (1997). Overexpression of Bcl‑2 inhibits alveolar cell apoptosis during involution and accelerates c‑myc−induced tumorigenesis of the mammary gland in transgenic mice. *Oncogene* **15**, 1787−1795.

[30] Ikegaki N, Katsumata M, Tsujimoto Y, Nakagawara A, and Brodeur GM (1995). Relationship between bcl‑2 and myc gene expression in human neuroblastoma. *Cancer Lett* **91**, 161−168.

[31] Shimada H, Stram DO, Chatten J, Joshi VV, Hachitanda Y, Brodeur GM, Lukens JN, Matthay KK, and Seeger RC (1995). Identification of subsets of neuroblastomas by combined histopathologic and N‑myc analysis. *J Natl Cancer Inst* **87**, 1470−1476.

[32] Weiss WA, Aldape K, Mohapatra G, Feuerstein BG, and Bishop JM (1997). Targeted expression of MYCN causes neuroblastoma in transgenic mice. *EMBO J* **16**, 2985−2995.

[33] Evan GI, Wyllie AH, Gilbert CS, Littlewood TD, Land H, Brooks M, Waters CM, Penn LZ, and Hancock DC (1992). Induction of apoptosis in fibroblasts by c‑myc protein. *Cell* **69**, 119−128.

[34] Cory S, Vaux DL, Strasser A, Harris AW, and Adams JM (1999). Insights from Bcl‑2 and Myc: malignancy involves abrogation of apoptosis as well as sustained proliferation. *Cancer Res* **59**, 1685s−1692s.

[35] Cole MD, and McMahon SB (1999). The Myc oncoprotein: a critical evaluation of transactivation and target gene regulation. *Oncogene* **18**, 2916−2924.

[36] Thompson EB (1998). The many roles of c‑Myc in apoptosis. *Annu Rev Physiol* **60**, 575−600.

[37] Daksis J, Lu RY, Facchini LM, Marhin WW, and Penn LJ (1994). Myc induces cyclin D1 expression in the absence of de novo protein synthesis and links mitogen‑stimulated signal transduction to the cell cycle. *Oncogene* **9**, 3635−3645.

[38] Meitar D, Crawford SE, Rademarker AW, and Cohn SV (1996). Tumor angiogenesis correlates with metastatic disease, N‑myc amplification, and poor outcome in human neuroblastoma. *J Clin Oncol* **14**, 405−414.

[39] Liu X, Turbyville T, Fritz A, and Whitesell L (1998). Inhibition of insulin‑like growth factor I receptor expression in neuroblastoma cells induces the regression of established tumors in mice. *Cancer Res* **58**, 5432−5438.

[40] Singleton J, Randolph A, and Feldman E (1996). Insulin‑like growth factor I receptor prevents apoptosis and enhances neuroblastoma tumorigenesis. *Cancer Res* **56**, 4522−4529.

[41] van Golen CM, Castle VP, and Feldman EV (2000). IGF‑I receptor activation and BCl‑2 overexpression prevent early apoptotic events in human neuroblastoma. *Cell Death Differ* **7**, 654−665.

[42] van Golen CM, and Feldman EV (2000). Insulin‑like growth factor I is the key factor in serum which protects neuroblastoma cells from hyperosmotic‑induced apoptosis. *J Cell Physiol* **182**, 24−32.

[43] Chambery D, Mohseni‑Zadeh S, de Galle B, and Babajko S (1999). N‑myc regulation of type I insulin‑like growth factor receptor in a human neuroblastoma cell line. *Cancer Res* **59**, 2898−2902.

[44] Misawa A, Hosoi H, Arimoto A, Shikata T, Akioka S, Matsumura T, Houghton PJ, and Sawada T (2000). N‑Myc induction stimulated by insulin‑like growth factor I through mitogen‑activated protein kinase signaling pathway in human neuroblastoma cells. *Cancer Res* **60**, 64−69.

[45] El‑Badry OM, Helman LJ, Chatten J, Steinberg SM, Evans AE, and Israel MA (1991). Insulin‑like growth factor II‑mediated proliferation of human neuroblastoma. *J Clin Invest* **87**, 648−657.